

# First application of the Oslo Method in inverse kinematics

## Nuclear level densities and $\gamma$ -ray strength functions of $^{87}\text{Kr}$

V. W. Ingeberg<sup>1</sup>, S. Siem<sup>1</sup>, M. Wiedeking<sup>2</sup>, K. Sieja<sup>3,4</sup>, D.L. Bleuel<sup>5</sup>, C.P. Brits<sup>2,6</sup>, T.D. Bucher<sup>2</sup>, T.S. Dinoko<sup>2</sup>, J.L. Easton<sup>2,7</sup>, A. Görzen<sup>1</sup>, M. Guttormsen<sup>1</sup>, P. Jones<sup>2</sup>, B.V. Kheswa<sup>2,8</sup>, N.A. Khumalo<sup>2</sup>, A.C. Larsen<sup>1</sup>, E.A. Lawrie<sup>2</sup>, J.J. Lawrie<sup>2</sup>, S.N.T. Majola<sup>2,9</sup>, K.L. Malatji<sup>2,6</sup>, L. Makhathini<sup>2,6</sup>, B. Maqabuka<sup>2,7</sup>, D. Negi<sup>2</sup>, S.P. Noncolela<sup>2,7</sup>, P. Papka<sup>2,6</sup>, E. Sahin<sup>1</sup>, R. Schwengner<sup>10</sup>, G.M. Tveten<sup>1</sup>, F. Zeiser<sup>1</sup>, and B.R. Zikhali<sup>2,9</sup>

<sup>1</sup> Department of Physics, University of Oslo, N-0316 Oslo, Norway iThemba LABS, P.O. Box 722, 7129 Somerset West, South Africa

<sup>2</sup> Université de Strasbourg, IPHC, 23 rue du Loess 67037 Strasbourg, France

<sup>3</sup> CNRS, UMR7178, 67037 Strasbourg, France

<sup>4</sup> Lawrence Livermore National Laboratory, 7000 East Avenue, Livermore, California 94550-9234, USA

<sup>5</sup> Department of Physics, Stellenbosch University, Private Bag X1, Matieland, 7602, South Africa

<sup>6</sup> Department of Physics, University of the Western Cape, P/B X17 Bellville 7535, South Africa

<sup>7</sup> Department of Physics, University of Johannesburg, P.O. Box 524, Auckland Park 2006, South Africa

<sup>8</sup> Department of Physics, University of Zululand, Private Bag X1001, KwaDlangezwa 3886, South Africa

<sup>9</sup> Institut für Strahlenphysik, Helmholtz-Zentrum Dresden-Rossendorf, 01328 Dresden, Germany

July 2019

**Abstract** The  $\gamma$ -ray strength function ( $\gamma$ SF) and nuclear level density (NLD) have been extracted for the first time from inverse kinematic reactions with the Oslo Method. This novel technique allows measurements of these properties across a wide range of previously inaccessible nuclei. Proton- $\gamma$  coincidence events from the  $d(^{86}\text{Kr}, p\gamma)^{87}\text{Kr}$  reaction were measured at iThemba LABS and the  $\gamma$ SF and NLD in  $^{87}\text{Kr}$  obtained. The nature of the low-energy region of the  $\gamma$ SF is explored through comparison to Shell Model calculations and is found to be dominated by M1 strength. The  $\gamma$ SF and NLD are used as input parameters to Hauser-Feshbach calculations to constrain  $(n, \gamma)$  cross sections of nuclei using the TALYS reaction code. These results are compared to  $^{86}\text{Kr}(n, \gamma)$  data from direct measurements.

**PACS.** 21.10.Ma Level density – 25.45.Hi Transfer reactions – 21.60.Cs Shell model – 21.10.Pc Single-particle levels and strength functions – 24.60.Dr Statistical compound-nucleus reactions

## 1 Introduction

The nuclear level density (NLD) and the  $\gamma$ -ray strength function ( $\gamma$ SF) are fundamental properties of the nucleus. The NLD was introduced by Bethe soon after the composition of nuclei was firmly established [1]. When excitation energy in a nucleus increases towards the particle separation energy, the NLD increases rapidly, creating a region referred to as the quasi-continuum. The ability of atomic nuclei to emit and absorb photons in the quasi-continuum is determined by the  $\gamma$ SF [2]. It is a measure of the average reduced  $\gamma$ -ray decay probability and reveals essential information about the electromagnetic response and therefore the nuclear structure of the nucleus.

With their significant applicability to astrophysical element formation via capture processes [3–6], NLDs and  $\gamma$ SFs have received increased experimental and theoretical

attention. They are also relevant to the design of existing and future nuclear power reactors, where reactor simulations depend on many evaluated nuclear reactions [7, 8]. The importance of NLDs and  $\gamma$ SFs is increasingly being recognized and efforts are currently underway to generate a reference database for  $\gamma$ SFs [9]. Nonetheless, challenges remain and nuclear physics properties, such as the NLD and  $\gamma$ SF, remain a main source of uncertainty in cross-section calculations. This is either due to the complete lack of experimental data or the associated large experimental uncertainties.

The situation can be improved through accurate experimental neutron capture cross sections, or indirectly by measuring NLD and  $\gamma$ SF data. One experimental approach, the Oslo Method [10], has been extensively used to measure the NLD and  $\gamma$ SF from particle- $\gamma$  coincident data. NLDs and  $\gamma$ SFs obtained with the Oslo Method have been shown to provide reliable neutron capture cross sections [11, 12] and proton capture cross sections [13]. In

Correspondence to: V. W. Ingeberg, e-mail: [vettlewi@fys.uio.no](mailto:vettlewi@fys.uio.no)

recent years, the Oslo Method has been extended to extract the  $\gamma$ SF and NLD following  $\beta$  decay [14]. Using  $\gamma$ SFs and NLDs to determine capture cross sections has several advantages since these properties can be obtained for any nucleus that can be populated in a reaction from which the excitation energy can be experimentally determined. Although the Oslo and  $\beta$ -Oslo Methods provide access to a vast range of stable and radioactive nuclei some species remain inaccessible. Many more nuclei become accessible by using inverse kinematic reactions, from radioactive species to several stable isotopes for which the manufacture of targets is problematic due to their chemical or physical properties.

In this Letter we report on the first application to measure the NLD and  $\gamma$ SF with the Oslo Method following an inverse kinematic reaction. This work lays the foundation of new opportunities to study statistical properties of nuclei, which were previously inaccessible, at stable and radioactive ion beam facilities. The results from the  $d(^{86}\text{Kr}, p)^{87}\text{Kr}$  reaction exhibit a low-energy enhancement of the  $\gamma$ SF in  $^{87}\text{Kr}$ , which is discussed in the context of Shell Model calculations. The  $^{86}\text{Kr}(n, \gamma)$  cross section is obtained from the TALYS reaction code [15] and compared to previous direct measurements to test the robustness of the experimental method.

## 2 Experiment

The experiment was performed with a 300 MeV  $^{86}\text{Kr}$  beam from the Separated Sector Cyclotron facility at iThemba LABS. Polyethylene targets with 99% deuteron enrichment were bombarded with a beam intensity of  $\approx 0.1$  pnA for 80 hrs. Several deuterated polyethylene targets, ranging in thicknesses from 110 to 550  $\mu\text{g}/\text{cm}^2$ , were used. Accounting for the target thicknesses the center-of-mass (CM) energy was 6.44(40) MeV. The reactions were identified through the detection of light charged particles in two silicon  $\Delta E$ -E telescopes covering scattering angles between  $24^\circ$  and  $67^\circ$  relative to the beam direction (corresponding to CM-angles  $38^\circ$  to  $121^\circ$ ). The E detectors were 1 mm thick while the  $\Delta E$  detectors were 0.3 and 0.5 mm thick. The dimensions of the W1-type double-sided silicon strip detectors [16] were  $4.8 \times 4.8$  cm and they consisted of 16 parallel and perpendicular strips 3 mm wide with an opening angle of  $\approx 1.5^\circ$  for each pixel. Suppression of  $\delta$  electrons was achieved by an aluminum foil of  $4.1 \text{ mg}/\text{cm}^2$  areal density which was placed in front of the  $\Delta E$  detectors. The  $\gamma$ -rays were measured with the AFRODITE array [17], which at the time of the experiment consisted of eight collimated and Compton suppressed high-purity germanium CLOVER-type detectors. Two non-collimated  $\text{LaBr}_3:\text{Ce}$  detectors ( $3.5'' \times 8''$ ) were coupled to the AFRODITE array and mounted 24 cm from the target at  $45^\circ$ . The detectors were calibrated using standard  $^{152}\text{Eu}$  and  $^{56}\text{Co}$  sources. The detector signals were processed by XIA digital electronics in time-stamped list mode with each channel self-triggered.

From the time-stamped data  $\text{particle} - \gamma$  events were constructed with an offline coincidence time window of

1850 ns. From double fold events, the  $p - \gamma$  coincidences were extracted by placing a gate on the protons in the particle identification spectrum. The selection of correlated events was made with a coincidence time of  $\sim 80$  ns by appropriately gating the prompt time peak. Contributions from uncorrelated events were subtracted from the data by placing off-prompt time gates. Approximately 100k proton- $\gamma$  events remained in both  $\text{LaBr}_3:\text{Ce}$  and CLOVER matrices. In this letter only the data from the  $\text{LaBr}_3:\text{Ce}$  detectors are included, although data from the CLOVER detectors yield similar results. Kinematic corrections due to the reaction Q-value, recoil energy of  $^{87}\text{Kr}$ , and the energy losses of the protons in the target and aluminum foils were applied to determine the excitation energy of the populated states. The experimental resolution of the excitation energy is of the order of  $\approx 500$  keV. The  $\gamma$ -rays in coincidence with protons were Doppler corrected by assuming the residual  $^{87}\text{Kr}$  nucleus not being deflected from the beam axis and has a constant velocity of 8.5% of c. Due to these assumptions the error in deflection angle is less than  $1.3^\circ$  while the error in velocity is less than 0.4% of c. These error are negligible as the major contributor to errors in the Doppler correction is the  $17^\circ$  opening angle of the  $\text{LaBr}_3:\text{Ce}$  detectors. This matrix is unfolded [18] with response functions of the detectors extracted from a Geant4 [19] simulation of the  $\text{LaBr}_3:\text{Ce}$  detectors. An iterative subtraction method, known as the First-Generation Method [20], is applied to the unfolded  $\gamma$ -ray spectra, revealing the distribution of primary  $\gamma$ -rays in each excitation bin (bin width 256 keV).

The NLD  $\rho(E_x)$  at excitation energy  $E_x$  and  $\gamma$ -ray transmission coefficient,  $\mathcal{T}(E_\gamma)$ , are related to the primary  $\gamma$ -ray spectrum by

$$P(E_x, E_\gamma) \propto \rho(E_x - E_\gamma) \mathcal{T}(E_\gamma), \quad (1)$$

and are extracted with a  $\chi^2$ -method [10] giving the unique solution of the functional shape of the NLD and  $\mathcal{T}(E_\gamma)$ . These are normalized to known experimental data to retrieve the correct slope and absolute value. The extraction has been performed within the limits  $3.2 < E_x < 5.2$  MeV and  $E_\gamma > 1.7$  MeV of the primary  $\gamma$ -ray matrix where statistical decay is observed to be dominant.

## 3 Normalization

From the primary  $\gamma$ -ray spectrum the NLD  $\tilde{\rho}(E_x)$  and  $\gamma$ -transmission coefficient  $\tilde{\mathcal{T}}(E_\gamma)$  are extracted. These are related to the physical solution by the following transformation:

$$\rho(E_x) = A \tilde{\rho}(E_x) e^{\alpha E_x} \quad (2)$$

$$\mathcal{T}(E_\gamma) = B \tilde{\mathcal{T}}(E_\gamma) e^{\alpha E_\gamma}, \quad (3)$$

where A and B are the absolute values and  $\alpha$  gives the slope.

For the level density, the slope and absolute value are determined by a fit to the level density found from the known discrete levels [21] at low-excitation energy and the

level density at the neutron separation energy ( $S_n = 5.5$  MeV) interpolated to the experimental data points with the constant temperature (CT) model [22]. The temperature is determined such that it minimizes

$$\chi^2 = \sum_i \left( \frac{\rho_i - \rho(E_i)}{\Delta\rho(E_i)} \right)^2, \quad (4)$$

where  $\rho_i$  is the level density found from known discrete levels for energies  $E_i < 2.4$  MeV and the constant temperature interpolation for energies  $E_i > 2.4$  MeV. The  $\rho(E_i)$  is given by Eqn.(2) and  $\Delta\rho(E_i)$  is the statistical and systematic uncertainties associated with the unfolding and first-generation method. The level density at  $S_n$  is determined from the average neutron resonance spacing [23] and is found to be 26.2(21) keV for s-wave resonances and 18.8(14) keV for  $J = 1/2$  p-wave resonances, giving a level density of 1/2 states of 91(5)  $\text{MeV}^{-1}$ . The total NLD at  $S_n$  is given by  $\rho(S_n) = \rho(S_n, 1/2)/g(S_n, 1/2)$  with a spin distribution

$$g(E, J) = \frac{2J+1}{2\sigma^2(E)} e^{-(J+1/2)^2/2\sigma^2(E)}. \quad (5)$$

The spin cutoff parameter  $\sigma(E)$  is modeled with the following energy dependence [11]

$$\sigma^2(E) = \sigma_d^2 + \frac{E - E_d}{S_n - E_d} (\sigma^2(S_n) - \sigma_d^2), \quad (6)$$

where  $E_d$  is the excitation energy below which the spin cutoff parameter  $\sigma = \sigma_d$  is a constant. The spin cutoff parameter  $\sigma_d$  at  $E_d \leq 2.4$  MeV is estimated to be 1.75, based on the spin assignment of the known levels, while the cut-off parameter at the neutron separation energy  $\sigma(S_n)$  is estimated to be 3.95, based on the estimate of the spin cut-off models of Refs. [22, 24, 25]. The uncertainty of  $\sigma(E)$  is estimated to be 15% for all relevant energies, giving a total NLD of 1472(427)  $\text{MeV}^{-1}$  at  $S_n$ . Since the reaction is sub-Coulomb barrier, most of the reactions are due to neutron capture following deuteron breakup in the Coulomb field of the  $^{86}\text{Kr}$  projectile. Thus the extracted level density in (1) needs to be weighted by a reduction factor

$$\rho_{\text{red}}(E_x - E_\gamma) = \rho_{\text{tot}}(E_x - E_\gamma) \times (g(E_x - E_\gamma, 1/2) + g(E_x - E_\gamma, 3/2)), \quad (7)$$

as 1/2 states seems to be strongly favoured in the initial population. This is accounted for in the determination of the normalization parameters and temperature by  $\rho_i \rightarrow \rho_i(g(E_i, 1/2) + g(E_i, 3/2))$  in eqn. (4). The total NLD is determined by  $\rho_{\text{tot}}(E_x) = \rho_{\text{red}}(E_x)/(g(E_i, 1/2) + g(E_i, 3/2))$ .

The absolute value of the transmission coefficients are normalized to the average radiative width of s-wave resonances  $\langle \Gamma_{\gamma 0} \rangle$  in a process detailed in [27], and converted to  $\gamma$ -SF by  $f(E_\gamma) = \mathcal{T}(E_\gamma)/(2\pi E_\gamma^3)$ . The value of  $\langle \Gamma_{\gamma 0} \rangle$  is estimated to be 0.25(10) eV based on the measured  $\Gamma_\gamma$  of s-wave resonances of [26]. All normalization parameters are listed in Table 1.

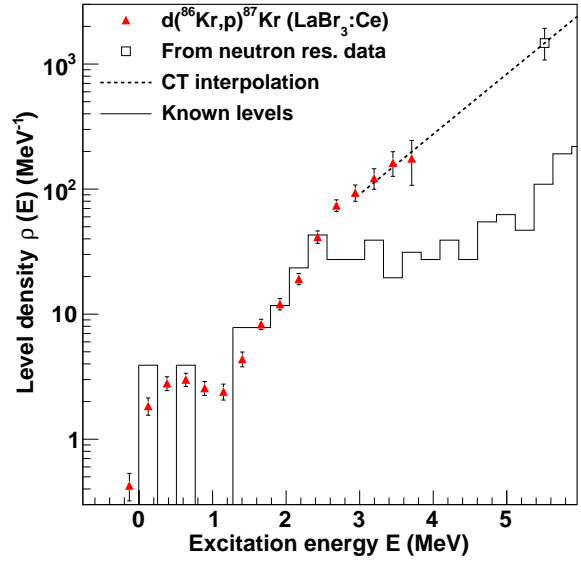


**Figure 1.** Normalized  $^{87}\text{Kr}$  nuclear level densities for  $\text{LaBr}_3:\text{Ce}$  (red circles) detectors. The black line shows the known levels while the open square is the level density at the neutron separation energy. The dashed line is the constant temperature interpolation. The error bars represent the upper and lower uncertainty limit due to all known statistical and systematic effects.

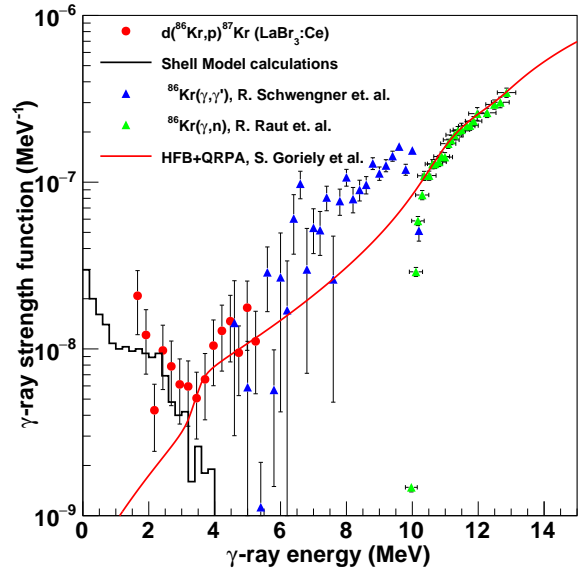


**Figure 2.**  $\gamma$ -ray strength function of  $^{87}\text{Kr}$  (red circles) compared with the  $\gamma$ -ray strength function of  $^{86}\text{Kr}$  extracted from  $^{86}\text{Kr}(\gamma, \gamma')$  (blue triangles) [28] and  $^{86}\text{Kr}(\gamma, n)$  (green squares) [29]. The solid black line are results from Shell Model calculations with a  $^{78}\text{Ni}$  core (see section 5 for details), while the red line is the microscopic HFB+QRPA prediction [30] for the E1 strength. The error bars include all known statistical and systematic errors.

**Table 1.** Parameters used in the normalization (see section 3 for details).

$D_0$	26.2(21) keV [23]
$D_1$ ( $J=1/2$ )	18.8(14) keV [23]
$\sigma(S_n)$	3.95(60)
$\sigma_d$	1.75(26)
$\rho(S_n, 1/2)$	91(5) MeV $^{-1}$
$\rho(S_n)$	1472(427) MeV $^{-1}$
$\langle \Gamma_{\gamma 0} \rangle$	0.25(10) eV [26]
$T$	0.9(1) MeV

## 4 Nuclear level densities and $\gamma$ -ray strength functions

The normalized NLD is shown in Figure 1 and is in excellent agreement with the constant temperature level density and matches well with the known discrete states at lower excitation energies. The normalized  $\gamma$ SF is shown in Figure 2 and is consistent with  $\gamma$ SFs from  $^{86}\text{Kr}(\gamma, \gamma')$  [28] and  $^{86}\text{Kr}(\gamma, n)$  [29], with the enhancement seen in the  $(\gamma, \gamma')$  data between 6 and 8 MeV caused by a Pygmy resonance [28]. A drop in the  $\gamma$ SFs at  $\sim 2.1$  MeV is caused by the 2123-keV state in  $^{87}\text{Kr}$ , which is strongly populated in the reaction, but less through feeding from the quasi-continuum. This causes the first generation method to over-subtract in the higher excitation-energy bins, causing an artificial drop in the  $\gamma$ SF. This effect has previously been discussed [31]. At low energies we observe a large enhancement in the  $\gamma$ SF, similar to what has been observed in several other nuclei [32–38]. Although the *upbend* has been independently confirmed [39], little is known of the origin of this feature, except that it is dominated by dipole radiation [40–42] and that it can have large effects on neutron capture cross sections [43].

## 5 Shell Model calculations

Calculations within the shell-model framework predicts the upbend due to M1 transitions [44]. In this work, large-scale shell-model calculations of the M1 component of the  $\gamma$ SF were performed in the model space outside the  $^{78}\text{Ni}$  core, containing  $f_{5/2}p_{3/2}p_{1/2}g_{9/2}$ -proton and  $d_{5/2}s_{1/2}d_{3/2}g_{7/2}h_{11/2}$ -neutron orbitals. The effective interaction employed here is described e.g. in Refs. [45, 46]. The diagonalization of the Hamiltonian matrix in the full configuration space was achieved using the Strasbourg shell-model code NATHAN [47]. The spin-part of the magnetic operator was quenched by a common factor of 0.75 [47]. We computed this way up to 60 states of each spin between 1/2 and 15/2 for both parities. This leads to a total of around  $8 \cdot 10^4$  M1 matrix elements, among which 14822 connect states located in the energy range  $E_x = 3.4 - 5.4$  MeV, as considered in the experiment. To obtain the average strength per energy interval,  $\langle B(M1) \rangle$ , the total transition strength was accumulated in 200 keV bins and divided by the number of transitions within these bins. The  $\gamma$ SF was obtained from the relation  $f_{M1}(E_\gamma, E_i, J_i, \pi) =$

$16\pi/9(\hbar c)^{-3}\langle B(M1)(E_\gamma, E_i, J_i, \pi) \rangle \rho(E_i, J_i, \pi)$ , where  $\rho_i(E_i, J_i, \pi)$  is the partial level density at the energy of the initial state ( $E_i$ ). The  $\gamma$ SF, shown in Figure 2, is an average of the  $f_{M1}s$  evaluated for each spin/parity separately. The shape of the shell-model  $\gamma$ SF is consistent with experimental data up to  $\sim 3$  MeV. Since the model space does not contain all spin-orbit partners (i.e.,  $\nu g_{9/2}$  and  $\pi f_{7/2}$  orbits) the strength above 4 MeV, due to the spin-flip transitions, can not be accounted for. However, the theoretical  $\gamma$ SF exhibits significant strength at  $E_\gamma = 0$ , as in the previous shell-model calculations in this mass region [44]. The largest  $B(M1)$  contributions at low  $\gamma$ -ray energies in  $^{87}\text{Kr}$  are related to transitions between close-lying negative-parity states with  $\nu d_{5/2} \otimes \pi f_{5/2}^{-1}g_{9/2}^1$  and  $\nu d_{5/2} \otimes \pi p_{3/2}^{-1}g_{9/2}^1$  components. The magnitude of the theoretical M1 strength is in good agreement with the data as measured in the experiment, however we cannot exclude an additional contribution from E1 strength. Recent experimental results in  $^{56}\text{Fe}$  [42] could suggest a mixture of M1 and E1 radiation in the enhancement region and the addition of a non-zero E1 component without an upbend towards  $E_\gamma \rightarrow 0$  MeV is predicted from Shell Model calculations [48]. Including the E1 strength calculations from the Hartree-Fock-Bogolyubov + QRPA (HFB+QRPA) model by [30] we observe an overall good agreement between theoretical predictions and experimental results.

## 6 Neutron capture cross sections

In a statistical framework the  $^{86}\text{Kr}(n, \gamma)$  cross section can be determined from the NLD,  $\gamma$ SF and a suitable neutron optical model potential (nOMP) for  $^{87}\text{Kr}$ . Phenomenological nOMPs e.g. from Ref. [49] are observed to give good agreement with the total cross section for nuclei close to the valley of stability. We performed Hauser-Feshbach (HF) [50] calculations with the TALYS<sup>1</sup> code [15], and the optical model potential of Ref. [49]. A semi-microscopic optical model [51] was also tested, and gave virtually the same results. Pre-equilibrium reactions were also taken into account. The  $^{87}\text{Kr}$  states used for the TALYS calculations are described by the known discrete states up to 2.3 MeV, and by the measured NLD above. Beyond 3.7 MeV the NLD is described by the CT model.

The measured  $\gamma$ SF are used as input between  $1.6 \leq E_\gamma \leq 5.2$  MeV (excluding the 2.1 MeV data point), as shown in Figure 2, for  $E_\gamma < 1.6$  MeV the results from the Shell Model calculations are used, while the results from microscopic HFB+QRPA calculations [30], as implemented in TALYS, of the E1 strength are used for  $E_\gamma > 5.2$  MeV. The M1 spin-flip contribution is also included as a standard Lorenzian with the TALYS parameterization. Figure 3 shows the resulting neutron capture cross section calculations. The input parameters have been varied in accordance with the statistical and systematic uncertainties to produce the red hashed error-band. We

<sup>1</sup> Version 1.9

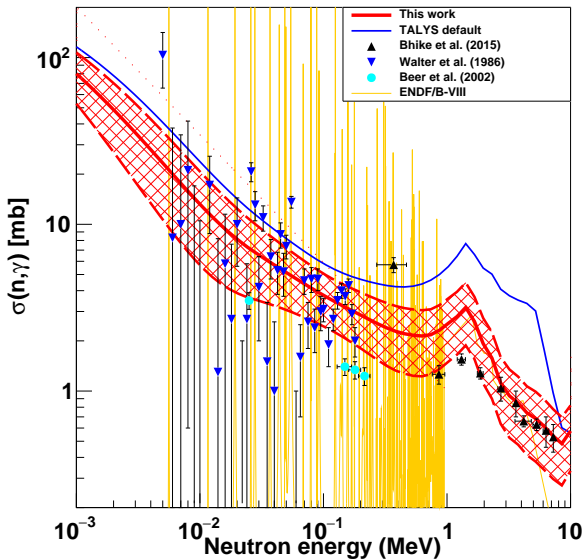


**Figure 3.**  $^{86}\text{Kr}(n, \gamma)$  cross sections. The red-hashed area represents the total uncertainty based on both systematical and statistic errors. The yellow and blue lines are from the evaluation of ENDF/B-VII.1 [7] and the TALYS default input, respectively, and is provided for comparison. The black triangles shows the direct measurements of Bhike *et al.* [53], the blue upside-down triangles are results from time-of-flight measurements of Walter *et al.* [52] and the turquoise circles are the results from the activation measurements of Beer *et al.* [54].

observe an overall good agreement with the direct measurements of Walter *et al.* [52] and Bhike *et al.* [53], while somewhat high compared with the activation results of Beer *et al.* [54]. The Maxwellian average (MACS) at the typical s-process temperature of 30 keV is found to be 7.6(49) mb, which is higher than the evaluated value of 3.4(3) mb found in KaDoNis [55]. This discrepancy can be explained by the fact that HF calculations will give results that overestimate the MACS for low temperatures when the level density is low [56]. A possible resolution could be the emerging “High Fidelity Resonance” method [57, 58].

## 7 Conclusion

We have presented a novel method for obtaining  $\gamma$ SF and NLD using inverse kinematic reactions, which opens opportunities to study a wide range of stable and radioactive nuclei. The  $d(^{86}\text{Kr}, p\gamma)$  reaction was used to measure the NLD and  $\gamma$ SF in  $^{87}\text{Kr}$ . The low-energy part of the  $\gamma$ SF is found to exhibit an enhancement. Shell Model calculations were performed and suggest that the enhancement is predominantly due to low-energy M1 transitions in  $^{87}\text{Kr}$ .

The  $\gamma$ SF and NLD measurements in  $^{87}\text{Kr}$  were used to calculate  $(n, \gamma)$  cross sections, which are in good agreement with those from direct measurements, and give confidence in the approach using inverse kinematic reactions.

This is consistent with the findings of previous work with the Oslo Method and is particularly interesting since direct measurement of neutron capture cross sections over a wide range of incident neutron energies is very challenging. It is clear that  $\gamma$ SFs and NLDs provide a viable alternative to obtain reliable capture cross sections.

With the Inverse-Oslo Method, new regions of the nuclear chart become accessible to experiments, which also brings about new challenges. For exotic nuclei, neutron resonance data are not known and the normalizing procedure needs to be revised. One possibility is that the slope of the  $\gamma$ SF, and thereby also the slope of the NLD, could be constrained using the Ratio Method [39], leaving the absolute value of the NLD to be determined by the known discrete levels. Unfortunately, this still does not determine the absolute value of the  $\gamma$ SF. However, reasonable estimates of the absolute value may be obtained from systematics of the  $\langle \Gamma_{\gamma 0} \rangle$ .

Measuring statistical properties of nuclei from inverse kinematic reactions provides a novel and complementary foundation for exploring the limitations of the current models of statistical behavior in the nucleus. It will allow to further constrain the uncertainties in models which are used in nuclear astrophysics and reactor physics.

The authors would like to thank iThemba LABS operations for stable running conditions and John Greene (Argonne National Lab.) for providing excellent targets. This work is based on research supported by the Research Council of Norway under project Grants No. 222287, 262952 (G.M.T), 263030 (V.W.I, S.S, A.G, F.Z) and 240104 (E.S), by the National Research Foundation of South Africa under grant no 118846, and the U.S. Department of Energy by Lawrence Livermore National Laboratory under Contract DE-AC52-07NA27344. A.C.L. gratefully acknowledges funding through ERC-STG-2014 Grant Agreement No. 637686, and support from the ChETEC Cost Action (CA16117) supported by COST. This work was performed within the IAEA CRP on “Updating the Photonuclear data Library and generating a Reference Database for Photon Strength Functions” (F410 32). M. W. and S. S. acknowledge the support from the IAEA under Research Contract 20454 and 20447, respectively.

## References

1. H. A. Bethe. An attempt to calculate the number of energy levels of a heavy nucleus. *Phys. Rev.*, 50:332–341, Aug 1936. doi: 10.1103/PhysRev.50.332. URL <https://link.aps.org/doi/10.1103/PhysRev.50.332>.
2. G. A. Bartholomew, E. D. Earle, A. J. Ferguson, J. W. Knowles, and M. A. Lone. *Gamma-Ray Strength Functions*, pages 229–324. Springer US, Boston, MA, 1973. ISBN 978-1-4615-9044-6. doi: 10.1007/978-1-4615-9044-6\_4. URL [http://dx.doi.org/10.1007/978-1-4615-9044-6\\_4](http://dx.doi.org/10.1007/978-1-4615-9044-6_4).
3. T Rauscher, N Dauphas, I Dillmann, C Fröhlich, Zs Fülöp, and Gy Gyürky. Constraining the astrophysical origin of the p-nuclei through nuclear physics

- and meteoritic data. *Reports on Progress in Physics*, 76(6):066201, 2013. URL <http://stacks.iop.org/0034-4885/76/i=6/a=066201>.
4. M. Arnould and S. Goriely. The p-process of stellar nucleosynthesis: astrophysics and nuclear physics status. *Physics Reports*, 384(1):1 – 84, 2003. ISSN 0370-1573. doi: [https://doi.org/10.1016/S0370-1573\(03\)00242-4](https://doi.org/10.1016/S0370-1573(03)00242-4). URL <http://www.sciencedirect.com/science/article/pii/S0370157303002424>.
  5. M. Arnould, S. Goriely, and K. Takahashi. The r-process of stellar nucleosynthesis: Astrophysics and nuclear physics achievements and mysteries. *Physics Reports*, 450(4):97 – 213, 2007. ISSN 0370-1573. doi: <https://doi.org/10.1016/j.physrep.2007.06.002>. URL <http://www.sciencedirect.com/science/article/pii/S0370157307002438>.
  6. S. Goriely. Radiative neutron captures by neutron-rich nuclei and the r-process nucleosynthesis. *Physics Letters B*, 436(1):10 – 18, 1998. ISSN 0370-2693. doi: [https://doi.org/10.1016/S0370-2693\(98\)00907-1](https://doi.org/10.1016/S0370-2693(98)00907-1). URL <http://www.sciencedirect.com/science/article/pii/S0370269398009071>.
  7. M.B. Chadwick, M. Herman, P. Obložinský, M.E. Dunn, Y. Danon, A.C. Kahler, D.L. Smith, B. Pritychenko, G. Arbanas, R. Arcilla, R. Brewer, D.A. Brown, R. Capote, A.D. Carlson, Y.S. Cho, H. Derrien, K. Guber, G.M. Hale, S. Hoblit, S. Holloway, T.D. Johnson, T. Kawano, B.C. Kiedrowski, H. Kim, S. Kunieda, N.M. Larson, L. Leal, J.P. Lestone, R.C. Little, E.A. McCutchan, R.E. MacFarlane, M. MacInnes, C.M. Mattoon, R.D. McKnight, S.F. Mughabghab, G.P.A. Nobre, G. Palmiotti, A. Palumbo, M.T. Pigni, V.G. Pronyaev, R.O. Sayer, A.A. Sonzogni, N.C. Summers, P. Talou, I.J. Thompson, A. Trkov, R.L. Vogt, S.C. van der Marck, A. Wallner, M.C. White, D. Wiarda, and P.G. Young. Endf/b-vii.1 nuclear data for science and technology: Cross sections, covariances, fission product yields and decay data. *Nuclear Data Sheets*, 112(12):2887 – 2996, 2011. ISSN 0090-3752. doi: <https://doi.org/10.1016/j.nds.2011.11.002>. URL <http://www.sciencedirect.com/science/article/pii/S009037521100113X>. Special Issue on ENDF/B-VII.1 Library.
  8. M.B. Chadwick. Report of the nuclear physics and related computational science r&d for advanced fuel cycles workshop, August 2006.
  9. Dimitriou, Paraskevi, Firestone, Richard B., Siem, Sunniva, Becvár, Frantisek, Krticka, Milan, Varlamov, Vladimir V., and Wiedeking, Mathis. Updated photonuclear data library and database for photon strength functions. *EPJ Web of Conferences*, 93:06004, 2015. doi: 10.1051/epjconf/20159306004. URL <https://doi.org/10.1051/epjconf/20159306004>.
  10. A Schiller, L Bergholt, M Guttormsen, E Melby, J Rekstad, and S Siem. Extraction of level density and  $\gamma$  strength function from primary  $\gamma$  spectra. *Nucl. Instrum. Methods Phys. Res., Sect. A*, 447(3):498–511, jun 2000. ISSN 01689002. doi: 10.1016/S0168-9002(99)01187-0. URL [https://dx.doi.org/10.1016/S0168-9002\(99\)01187-0](https://dx.doi.org/10.1016/S0168-9002(99)01187-0).
  11. M. Guttormsen, S. Goriely, A. C. Larsen, A. Görzen, T. W. Hagen, T. Renstrøm, S. Siem, N. U. H. Syed, G. Tagliente, H. K. Toft, H. Utsunomiya, A. V. Voinov, and K. Wikan. Quasicontinuum  $\gamma$  decay of  $^{91,92}\text{Zr}$ : Benchmarking indirect  $(n, \gamma)$  cross section measurements for the s process. *Phys. Rev. C*, 96:024313, Aug 2017. doi: 10.1103/PhysRevC.96.024313. URL <https://link.aps.org/doi/10.1103/PhysRevC.96.024313>.
  12. B. V. Kheswa, M. Wiedeking, J. A. Brown, A. C. Larsen, S. Goriely, M. Guttormsen, F. L. Bello Garrote, L. A. Bernstein, D. L. Bleuel, T. K. Eriksen, F. Giacoppo, A. Görzen, B. L. Goldblum, T. W. Hagen, P. E. Koehler, M. Klintefjord, K. L. Malatji, J. E. Midtbø, H. T. Nyhus, P. Papka, T. Renstrøm, S. J. Rose, E. Sahin, S. Siem, and T. G. Tornyi.  $^{137,138,139}\text{La}(n, \gamma)$ . *Phys. Rev. C*, 95:045805, Apr 2017. doi: 10.1103/PhysRevC.95.045805. URL <https://link.aps.org/doi/10.1103/PhysRevC.95.045805>.
  13. A. C. Larsen, M. Guttormsen, R. Schwengner, D. L. Bleuel, S. Goriely, S. Harissopoulos, F. L. Bello Garrote, Y. Byun, T. K. Eriksen, F. Giacoppo, A. Görzen, T. W. Hagen, M. Klintefjord, T. Renstrøm, S. J. Rose, E. Sahin, S. Siem, T. G. Tornyi, G. M. Tveten, A. V. Voinov, and M. Wiedeking. Experimentally constrained  $(p, \gamma)^{89}\text{Y}$  and  $(n, \gamma)^{89}\text{Y}$  reaction rates relevant to p-process nucleosynthesis. *Phys. Rev. C*, 93:045810, Apr 2016. doi: 10.1103/PhysRevC.93.045810. URL <http://link.aps.org/doi/10.1103/PhysRevC.93.045810>.
  14. S. N. Liddick, A. Spyrou, B. P. Crider, F. Naqvi, A. C. Larsen, M. Guttormsen, M. Mumpower, R. Surman, G. Perdikakis, D. L. Bleuel, A. Couture, L. Crespo Campo, A. C. Dombos, R. Lewis, S. Mosby, S. Nikas, C. J. Prokop, T. Renstrom, B. Rubio, S. Siem, and S. J. Quinn. Experimental neutron capture rate constraint far from stability. *Phys. Rev. Lett.*, 116:242502, Jun 2016. doi: 10.1103/PhysRevLett.116.242502. URL <http://link.aps.org/doi/10.1103/PhysRevLett.116.242502>.
  15. A. J. Koning, S. Hilaire, and M. C. Duijvestijn. Talys-1.0. In *International Conference on Nuclear Data for Science and Technology 2007*, pages 2–5, Les Ulis, France, may 2008. EDP Sciences. doi: 10.1051/ndata:07767. URL <http://nd2007.edpsciences.org/10.1051/ndata:07767>.
  16. Micron Semiconductor Ltd. Product catalogue. Technical report, Micron Semiconductor Ltd., 2017. URL <http://micronsemiconductor.co.uk/wp-content/uploads/2017/01/cat.pdf>.
  17. M. Lipoglavšek, A. Likar, M. Vencelj, T. Vidmar, R.A. Bark, E. Gueorguieva, F. Komati, J.J. Lawrie, S.M. Maliage, S.M. Mullins, S.H.T. Murray, and T.M. Rashashidzha. Measuring high-energy  $\gamma$ -rays with ge clover detectors. *Nuclear Instruments and Methods in Physics Research Section A: Accelerators, Spectrometers, Detectors and Associated Equipment*, 550(1-2):160–164, 2005. doi: 10.1016/j.nima.2005.02.060.

- ters, *Detectors and Associated Equipment*, 557(2):523 – 527, 2006. ISSN 0168-9002. doi: 10.1016/j.nima.2005.11.067. URL <http://www.sciencedirect.com/science/article/pii/S0168900205021935>.
18. M Guttormsen, T.S Tveter, L Bergholt, F Ingebretsen, and J Rekstad. The unfolding of continuum  $\gamma$ -ray spectra. *Nucl. Instrum. Methods Phys. Res., Sect. A*, 374(3):371–376, jun 1996. ISSN 01689002. doi: 10.1016/0168-9002(96)00197-0. URL [https://dx.doi.org/10.1016/0168-9002\(96\)00197-0](https://dx.doi.org/10.1016/0168-9002(96)00197-0).
  19. S. Agostinelli, J. Allison, K. Amako, J. Apostolakis, H. Araujo, P. Arce, M. Asai, D. Axen, S. Banerjee, G. Barrand, F. Behner, L. Bellagamba, J. Boudreau, L. Broglia, A. Brunengo, H. Burkhardt, S. Chauvie, J. Chuma, R. Chytracek, G. Cooperman, G. Cosmo, P. Degtyarenko, A. Dell'Acqua, G. Depaola, D. Dietrich, R. Enami, A. Feliciello, C. Ferguson, H. Fesefeldt, G. Folger, F. Foppiano, A. Forti, S. Garelli, S. Giani, R. Giannitrapani, D. Gibin, J.J. Gómez Cadenas, I. González, G. Gracia Abril, G. Greeniaus, W. Greiner, V. Grichine, A. Grossheim, S. Guatelli, P. Gumplinger, R. Hamatsu, K. Hashimoto, H. Hasui, A. Heikkinen, A. Howard, V. Ivanchenko, A. Johnson, F.W. Jones, J. Kallenbach, N. Kanaya, M. Kawabata, Y. Kawabata, M. Kawaguti, S. Kelner, P. Kent, A. Kimura, T. Kodama, R. Kokoulin, M. Kossov, H. Kurashige, E. Lamanna, T. Lampén, V. Lara, V. Lefebure, F. Lei, M. Liendl, W. Lockman, F. Longo, S. Magni, M. Maire, E. Medernach, K. Minamimoto, P. Mora de Freitas, Y. Morita, K. Murakami, M. Nagamatu, R. Nartallo, P. Nieminen, T. Nishimura, K. Ohtsubo, M. Okamura, S. O'Neale, Y. Oohata, K. Paech, J. Perl, A. Pfeiffer, M.G. Pia, F. Ranjard, A. Rybin, S. Sadilov, E. Di Salvo, G. Santin, T. Sasaki, N. Savvas, Y. Sawada, S. Scherer, S. Sei, V. Sirotenko, D. Smith, N. Starkov, H. Stoecker, J. Sulkimo, M. Takahata, S. Tanaka, E. Tcherniaev, E. Safai Tehrani, M. Tropeano, P. Truscott, H. Uno, L. Urban, P. Urban, M. Verderi, A. Walkden, W. Wander, H. Weber, J.P. Wellisch, T. Wenaus, D.C. Williams, D. Wright, T. Yamada, H. Yoshida, and D. Zschiesche. Geant4—a simulation toolkit. *Nuclear Instruments and Methods in Physics Research Section A: Accelerators, Spectrometers, Detectors and Associated Equipment*, 506(3):250 – 303, 2003. ISSN 0168-9002. doi: 10.1016/S0168-9002(03)01368-8. URL <http://www.sciencedirect.com/science/article/pii/S0168900203013688>.
  20. M. Guttormsen, T. Ramsøy, and J. Rekstad. The first generation of  $\gamma$ -rays from hot nuclei. *Nucl. Instrum. Methods Phys. Res., Sect. A*, 255(3):518–523, apr 1987. ISSN 01689002. doi: 10.1016/0168-9002(87)91221-6. URL [https://dx.doi.org/10.1016/0168-9002\(87\)91221-6](https://dx.doi.org/10.1016/0168-9002(87)91221-6).
  21. T.D. Johnson and W.D. Kulp. Nuclear data sheets for  $a = 87$ . *Nuclear Data Sheets*, 129:1 – 190, 2015. ISSN 0090-3752. doi: 10.1016/j.nds.2015.09.001. URL <http://www.sciencedirect.com/science/article/pii/S0090375215000460>.
  22. A. Glibert and A. G. W. Cameron. A composite nuclear-level density formula with shell corrections. *Can. J. Phys.*, 43:1446–1496, 1965. doi: 10.1139/p65-139. URL <http://dx.doi.org/10.1139/p65-139>.
  23. R. F. Carlton, R. R. Winters, C. H. Johnson, N. W. Hill, and J. A. Harvey. Total cross section and resonance spectroscopy for  $n + ^{86}\text{Kr}$ . *Phys. Rev. C*, 38: 1605–1618, Oct 1988. doi: 10.1103/PhysRevC.38.1605. URL <https://link.aps.org/doi/10.1103/PhysRevC.38.1605>.
  24. Till von Egidy and Dorel Bucurescu. Systematics of nuclear level density parameters. *Phys. Rev. C*, 72:044311, Oct 2005. doi: 10.1103/PhysRevC.72.044311. URL <https://link.aps.org/doi/10.1103/PhysRevC.72.044311>.
  25. T. von Egidy and D. Bucurescu. Experimental energy-dependent nuclear spin distributions. *Phys. Rev. C*, 80:054310, Nov 2009. doi: 10.1103/PhysRevC.80.054310. URL <https://link.aps.org/doi/10.1103/PhysRevC.80.054310>.
  26. S. Raman, B. Fogelberg, J. A. Harvey, R. L. Macklin, P. H. Stelson, A. Schröder, and K. L. Kratz. Overlapping  $\beta$  decay and resonance neutron spectroscopy of levels in  $^{87}\text{Kr}$ . *Phys. Rev. C*, 28:602–622, Aug 1983. doi: 10.1103/PhysRevC.28.602. URL <https://link.aps.org/doi/10.1103/PhysRevC.28.602>.
  27. A. Voinov, M. Guttormsen, E. Melby, J. Rekstad, A. Schiller, and S. Siem.  $\gamma$ . *Phys. Rev. C*, 63:044313, Mar 2001. doi: 10.1103/PhysRevC.63.044313. URL <https://link.aps.org/doi/10.1103/PhysRevC.63.044313>.
  28. R. Schwengner, R. Massarczyk, G. Rusev, N. Tsoneva, D. Bemmerer, R. Beyer, R. Hannaske, A. R. Jung-hans, J. H. Kelley, E. Kwan, H. Lenske, M. Marta, R. Raut, K. D. Schilling, A. Tonchev, W. Tornow, and A. Wagner. Pygmy dipole strength in  $^{86}\text{Kr}$  and systematics of  $n = 50$  isotones. *Phys. Rev. C*, 87:024306, Feb 2013. doi: 10.1103/PhysRevC.87.024306. URL <https://link.aps.org/doi/10.1103/PhysRevC.87.024306>.
  29. R. Raut, A. P. Tonchev, G. Rusev, W. Tornow, C. Iliadis, M. Lugaro, J. Buntain, S. Goriely, J. H. Kelley, R. Schwengner, A. Banu, and N. Tsoneva. Cross-section measurements of the  $^{86}\text{Kr}(\gamma, n)$  reaction to probe the  $s$ -process branching at  $^{85}\text{Kr}$ . *Phys. Rev. Lett.*, 111:112501, Sep 2013. doi: 10.1103/PhysRevLett.111.112501. URL <https://link.aps.org/doi/10.1103/PhysRevLett.111.112501>.
  30. S. Goriely, E. Khan, and M. Samyn. Microscopic hfb + qrpa predictions of dipole strength for astrophysics applications. *Nuclear Physics A*, 739(3):331 – 352, 2004. ISSN 0375-9474. doi: <https://doi.org/10.1016/j.nuclphysa.2004.04.105>. URL <http://www.sciencedirect.com/science/article/pii/S0375947404006578>.
  31. A. C. Larsen, M. Guttormsen, M. Krtička, E. Běták, A. Bürger, A. Görgen, H. T. Nyhus, J. Rekstad, A. Schiller, S. Siem, H. K. Toft, G. M. Tveten, A. V.

- Voinov, and K. Wikan. Analysis of possible systematic errors in the oslo method. *Phys. Rev. C*, 83:034315, Mar 2011. doi: 10.1103/PhysRevC.83.034315. URL <https://link.aps.org/doi/10.1103/PhysRevC.83.034315>.
32. T. Renstrøm, H.-T. Nyhus, H. Utsunomiya, R. Schwengner, S. Goriely, A. C. Larsen, D. M. Filipescu, I. Gheorghe, L. A. Bernstein, D. L. Bleuel, T. Glodariu, A. Görgen, M. Guttormsen, T. W. Hagen, B. V. Kheswa, Y.-W. Lui, D. Negi, I. E. Ruud, T. Shima, S. Siem, K. Takahisa, O. Tesileanu, T. G. Tornyi, G. M. Tveten, and M. Wiedeking. Low-energy enhancement in the  $\gamma$ -ray strength functions of  $^{73,74}\text{Ge}$ . *Phys. Rev. C*, 93:064302, Jun 2016. doi: 10.1103/PhysRevC.93.064302. URL <http://link.aps.org/doi/10.1103/PhysRevC.93.064302>.
33. M. Guttormsen, R. Chankova, U. Agvaanluvsan, E. Algin, L. A. Bernstein, F. Ingebretsen, T. Lönnroth, S. Messelt, G. E. Mitchell, J. Rekstad, A. Schiller, S. Siem, A. C. Sunde, A. Voinov, and S. Ødegård. Radiative strength functions in  $^{93-98}\text{Mo}$ . *Phys. Rev. C*, 71:044307, Apr 2005. doi: 10.1103/PhysRevC.71.044307. URL <http://link.aps.org/doi/10.1103/PhysRevC.71.044307>.
34. A. C. Larsen, R. Chankova, M. Guttormsen, F. Ingebretsen, S. Messelt, J. Rekstad, S. Siem, N. U. H. Syed, S. W. Ødegård, T. Lönnroth, A. Schiller, and A. Voinov. Microcanonical entropies and radiative strength functions of  $^{50,51}\text{V}$ . *Phys. Rev. C*, 73:064301, Jun 2006. doi: 10.1103/PhysRevC.73.064301. URL <http://link.aps.org/doi/10.1103/PhysRevC.73.064301>.
35. N. U. H. Syed, A. C. Larsen, A. Bürger, M. Guttormsen, S. Harissopoulos, M. Kmiecik, T. Konstantinopoulos, M. Krtička, A. Lagoyannis, T. Lönnroth, K. Mazurek, M. Norby, H. T. Nyhus, G. Perdikakis, S. Siem, and A. Spyrou. Extraction of thermal and electromagnetic properties in  $^{45}\text{Ti}$ . *Phys. Rev. C*, 80:044309, Oct 2009. doi: 10.1103/PhysRevC.80.044309. URL <http://link.aps.org/doi/10.1103/PhysRevC.80.044309>.
36. A. C. Larsen, I. E. Ruud, A. Bürger, S. Goriely, M. Guttormsen, A. Görgen, T. W. Hagen, S. Harissopoulos, H. T. Nyhus, T. Renstrøm, A. Schiller, S. Siem, G. M. Tveten, A. Voinov, and M. Wiedeking. Transitional  $\gamma$  strength in cd isotopes. *Phys. Rev. C*, 87:014319, Jan 2013. doi: 10.1103/PhysRevC.87.014319. URL <http://link.aps.org/doi/10.1103/PhysRevC.87.014319>.
37. A. Simon, M. Guttormsen, A. C. Larsen, C. W. Beausang, P. Humby, J. T. Burke, R. J. Casperson, R. O. Hughes, T. J. Ross, J. M. Allmond, R. Chyzh, M. Dag, J. Koglin, E. McCleskey, M. McCleskey, S. Ota, and A. Saastamoinen. First observation of low-energy  $\gamma$ -ray enhancement in the rare-earth region. *Phys. Rev. C*, 93:034303, Mar 2016. doi: 10.1103/PhysRevC.93.034303. URL <http://link.aps.org/doi/10.1103/PhysRevC.93.034303>.
38. B. V. Kheswa, M. Wiedeking, F. Giacoppo, S. Goriely, M. Guttormsen, A.C. Larsen, F.L. Bello Garrote, T.K. Eriksen, A. Görgen, T.W. Hagen, P.E. Koehler, M. Klintefjord, H.T. Nyhus, P. Papka, T. Renstrøm, S. Rose, E. Sahin, S. Siem, and T. Tornyi. Galactic production of  $^{138}\text{La}$ : Impact of  $^{138,139}\text{La}$  statistical properties. *Phys. Lett. B*, 744:268 – 272, 2015. ISSN 0370-2693. doi: 10.1016/j.physletb.2015.03.065. URL <http://www.sciencedirect.com/science/article/pii/S0370269315002403>.
39. M. Wiedeking, L. A. Bernstein, M. Krtička, D. L. Bleuel, J. M. Allmond, M. S. Basunia, J. T. Burke, P. Fallon, R. B. Firestone, B. L. Goldblum, R. Hatarik, P. T. Lake, I-Y. Lee, S. R. Lesser, S. Paschalis, M. Petri, L. Phair, and N. D. Scielzo. Low-energy enhancement in the photon strength of  $^{95}\text{Mo}$ . *Phys. Rev. Lett.*, 108:162503, Apr 2012. doi: 10.1103/PhysRevLett.108.162503. URL <http://link.aps.org/doi/10.1103/PhysRevLett.108.162503>.
40. A. C. Larsen, N. Blasi, A. Bracco, F. Camera, T. K. Eriksen, A. Görgen, M. Guttormsen, T. W. Hagen, S. Leoni, B. Million, H. T. Nyhus, T. Renstrøm, S. J. Rose, I. E. Ruud, S. Siem, T. Tornyi, G. M. Tveten, A. V. Voinov, and M. Wiedeking. Evidence for the dipole nature of the low-energy  $\gamma$  enhancement in  $^{56}\text{Fe}$ . *Phys. Rev. Lett.*, 111:242504, Dec 2013. doi: 10.1103/PhysRevLett.111.242504. URL <http://link.aps.org/doi/10.1103/PhysRevLett.111.242504>.
41. A C Larsen, M Guttormsen, N Blasi, A Bracco, F Camera, L Crespo Campo, T K Eriksen, A Görgen, T W Hagen, V W Ingeberg, B V Kheswa, S Leoni, J E Midtbø, B Million, H T Nyhus, T Renstrøm, S J Rose, I E Ruud, S Siem, T G Tornyi, G M Tveten, A V Voinov, M Wiedeking, and F Zeiser. Low-energy enhancement and fluctuations of  $\gamma$ -ray strength functions in  $^{56,57}\text{Fe}$ : test of the brink–axel hypothesis. *Jour. Phys. G Nucl. and Part. Phys.*, 44(6):064005, 2017. URL <http://stacks.iop.org/0954-3899/44/i=6/a=064005>.
42. M. D. Jones, A. O. Macchiavelli, M. Wiedeking, L. A. Bernstein, H. L. Crawford, C. M. Campbell, R. M. Clark, M. Cromaz, P. Fallon, I. Y. Lee, M. Salatene, A. Wiens, A. D. Ayangeakaa, D. L. Bleuel, S. Bottoni, M. P. Carpenter, H. M. Davids, J. Elson, A. Görgen, M. Guttormsen, R. V. F. Janssens, J. E. Kinnison, L. Kirsch, A. C. Larsen, T. Lauritsen, W. Revol, D. G. Sarantites, S. Siem, A. V. Voinov, and S. Zhu. Examination of the low-energy enhancement of the  $\gamma$ -ray strength function of  $^{56}\text{Fe}$ . *Phys. Rev. C*, 97:024327, Feb 2018. doi: 10.1103/PhysRevC.97.024327. URL <https://link.aps.org/doi/10.1103/PhysRevC.97.024327>.
43. A. C. Larsen and S. Goriely. Impact of a low-energy enhancement in the  $\gamma$ -ray strength function on the neutron-capture cross section. *Phys. Rev. C*, 82:014318, Jul 2010. doi: 10.1103/PhysRevC.82.014318. URL <http://link.aps.org/doi/10.1103/PhysRevC.82.014318>.

44. R. Schwengner, S. Frauendorf, and A. C. Larsen. Low-energy enhancement of magnetic dipole radiation. *Phys. Rev. Lett.*, 111:232504, Dec 2013. doi: 10.1103/PhysRevLett.111.232504. URL <https://link.aps.org/doi/10.1103/PhysRevLett.111.232504>.
45. M. Czerwiński, T. Rząca-Urban, W. Urban, P. Baczyk, K. Sieja, B. M. Nyakó, J. Timár, I. Kuti, T. G. Tornyi, L. Atanasova, A. Blanc, M. Jentschel, P. Mutti, U. Köster, T. Soldner, G. de France, G. S. Simpson, and C. A. Ur. Neutron-proton multiplets in the nucleus  $^{88}\text{Br}$ . *Phys. Rev. C*, 92:014328, Jul 2015. doi: 10.1103/PhysRevC.92.014328. URL <https://link.aps.org/doi/10.1103/PhysRevC.92.014328>.
46. J. Litzinger, A. Blazhev, A. Dewald, F. Didierjean, G. Duchêne, C. Fransen, R. Lozeva, K. Sieja, D. Verney, G. de Angelis, D. Bazzacco, B. Birkenbach, S. Bottoni, A. Bracco, T. Braunroth, B. Cederwall, L. Corradi, F. C. L. Crespi, P. Désesquelles, J. Eberth, E. Ellinger, E. Farnea, E. Fioretto, R. Gernhäuser, A. Goasduff, A. Görgen, A. Gottardo, J. Grebosz, M. Hackstein, H. Hess, F. Ibrahim, J. Jolie, A. Jungclaus, K. Kolos, W. Korten, S. Leoni, S. Lunardi, A. Maj, R. Menegazzo, D. Mengoni, C. Michelagnoli, T. Mijatovic, B. Million, O. Möller, V. Modamio, G. Montagnoli, D. Montanari, A. I. Morales, D. R. Napoli, M. Niikura, G. Pollarolo, A. Pullia, B. Quintana, F. Recchia, P. Reiter, D. Rosso, E. Sahin, M. D. Salsac, F. Scarlassara, P.-A. Söderström, A. M. Stefanini, O. Stezowski, S. Szilner, Ch. Theisen, J. J. Valiente Dobón, V. Vandone, and A. Vogt. Transition probabilities in neutron-rich  $^{84,86}\text{Se}$ . *Phys. Rev. C*, 92:064322, Dec 2015. doi: 10.1103/PhysRevC.92.064322. URL <https://link.aps.org/doi/10.1103/PhysRevC.92.064322>.
47. E. Caurier, G. Martínez-Pinedo, F. Nowacki, A. Poves, and A. P. Zuker. The shell model as a unified view of nuclear structure. *Rev. Mod. Phys.*, 77:427–488, Jun 2005. doi: 10.1103/RevModPhys.77.427. URL <https://link.aps.org/doi/10.1103/RevModPhys.77.427>.
48. K. Sieja. Electric and magnetic dipole strength at low energy. *Phys. Rev. Lett.*, 119:052502, Jul 2017. doi: 10.1103/PhysRevLett.119.052502. URL <https://link.aps.org/doi/10.1103/PhysRevLett.119.052502>.
49. A.J. Koning and J.P. Delaroche. Local and global nucleon optical models from 1 kev to 200 mev. *Nucl. Phys. A*, 713(3):231 – 310, 2003. ISSN 0375-9474. doi: 10.1016/S0375-9474(02)01321-0. URL <https://www.sciencedirect.com/science/article/pii/S0375947402013210>.
50. Walter Hauser and Herman Feshbach. The inelastic scattering of neutrons. *Phys. Rev.*, 87:366–373, Jul 1952. doi: 10.1103/PhysRev.87.366. URL <https://link.aps.org/doi/10.1103/PhysRev.87.366>.
51. E. Bauge, J. P. Delaroche, and M. Girod. Lane-consistent, semimicroscopic nucleon-nucleus optical model. *Phys. Rev. C*, 63:024607, Jan 2001. doi: 10.1103/PhysRevC.63.024607. URL <https://link.aps.org/doi/10.1103/PhysRevC.63.024607>.
52. G. Walter, B. Leugers, F. Käppeler, Z. Y. Bao, G. Reffo, and F. Fabbri. Kilo-electron-volt neutron capture cross sections of the krypton isotopes. *Nuclear Science and Engineering*, 93:357–369, 1986. doi: 10.13182/NSE86-A18471. URL <http://dx.doi.org/10.13182/NSE86-A18471>.
53. Megha Bhike, E. Rubino, M. E. Gooden, Krishchayan, and W. Tornow. Measurements of the  $^{86}\text{Kr}(n, \gamma)^{87}\text{Kr}$  and  $^{86}\text{Kr}(n, 2n)^{85}\text{Kr}^m$  reaction cross sections below  $E_n = 15$  mev. *Phys. Rev. C*, 92:014624, Jul 2015. doi: 10.1103/PhysRevC.92.014624. URL <http://link.aps.org/doi/10.1103/PhysRevC.92.014624>.
54. H. Beer, P. V. Sedyshev, W. Rochow, P. Mohr, and H. Oberhummer. Neutron capture measurements of the noble gas isotopes  $^{22}\text{Ne}$ ,  $^{40}\text{Ar}$  and  $^{78,80,84,86}\text{Kr}$  in the keV energy region. *Nuclear Physics A*, 705(1-2):239–261, jul 2002. ISSN 03759474. doi: 10.1016/S0375-9474(02)00645-0. URL <https://www.sciencedirect.com/science/article/abs/pii/S0375947402006450>.
55. I. Dillmann. Kadonis- the karlsruhe astrophysical database of nucleosynthesis in stars. *AIP Conf. Proc.*, 2006. doi: 10.1063/1.2187846. URL <http://dx.doi.org/10.1063/1.2187846>. online at <http://www.kadonis.org>.
56. Thomas Rauscher, Friedrich Karl Thielemann, and Karl Ludwig Kratz. Nuclear level density and the determination of thermonuclear rates for astrophysics. *Physical Review C - Nuclear Physics*, 56(3):1613–1625, sep 1997. ISSN 1089490X. doi: 10.1103/PhysRevC.56.1613. URL <https://link.aps.org/doi/10.1103/PhysRevC.56.1613>.
57. D. Rochman, A. J. Koning, J. Kopecky, J. C. Sublet, P. Ribon, and M. Moxon. From average parameters to statistical resolved resonances. *Annals of Nuclear Energy*, 51:60–68, jan 2013. ISSN 03064549. doi: 10.1016/j.anucene.2012.08.015. URL <https://www.sciencedirect.com/science/article/pii/S0306454912003350>.
58. D. Rochman, S. Goriely, A.J. Koning, and H. Ferroukhi. Radiative neutron capture: Hauser feshbach vs. statistical resonances. *Phys. Lett. B*, 764:109–113, Jan 2017. doi: 10.1016/j.physletb.2016.11.018. URL <http://dx.doi.org/10.1016/j.physletb.2016.11.018>.